Current models of receptor editing favor a return of self-reactive immature B cells to the pre-BII stage (*29*). Our observations indicate that the BCR regulates receptor editing by controlling the rate of B cell development. B cells with self-reactive antibodies and those cells that have not yet expressed a receptor are delayed in the RAG^+ small pre-BII cell compartment, where normal light chain rearrangement takes place. B cells expressing innocuous receptors transit rapidly from this stage to the immature compartment, where RAG gene expression and V(D)J recombination are down-regulated (*25, 26*). This new model clarifies how allelic exclusion is maintained in B cells despite high levels of receptor editing: B cells that deposit non–self-reactive antibodies on their cell surface rapidly turn off V(D)J recombination.

To estimate the extent of receptor replacement normally occurring in vivo, we combined the hCκ allele with three additional pre-rearranged Vκ-Jκ genes: 3-83κi, Vκ4R, and Vκ8R (*30, 31*). B cells that undergo receptor editing and replace the original mouse allele were enumerated by flow cytometry and mRNA analysis. Among these, $Igκ^{3\text{-}83/h}$ mice are unique in that replacement of the Vκ3-83 gene can be detected by loss of staining with a monoclonal antibody specific for Vκ3-83 (*32*). We found that about 25% of the B cells in $Igκ^{3\text{-}83/h}$ mice and 33% of the B cells in $Igκ^{Vκ4/h}$ mice substituted their light chains during B cell development (Fig. 3 and Table 1). $Igκ^{Vκ8/h}$ mice can only delete Vκ8R by RS recombination; nevertheless, 18% (±1) of B cells in these mice replaced the targeted gene and expressed hCκ or Igλ on the cell surface [Fig. 3 (*31*)]. Despite differences in the level of Ig κ chain editing, the amount of Igλ expression was similar in all strains (Figs. 2A and 3 and Table 1).

Our data from four separate Igκ knock-in mouse strains show that about 25% (±7) of the light chains found on the surface of developing B cells in vivo are produced by receptor editing. Whether all of these replacements are induced by self-reactivity is currently unknown. Nevertheless, extrapolating from these experiments, we conclude that receptor editing makes an important contribution to the normal antibody repertoire.

References and Notes

1. M. F. Burnet, *The Clonal Selection Theory of Acquired Immunity* (Cambridge Univ. Press, Cambridge, 1959).
2. D. Gay, T. Saunders, S. Camper, M. Weigert, *J. Exp. Med.* **177**, 999 (1993).
3. C. C. Goodnow *et al.*, *Nature* **334**, 676 (1988).
4. D. A. Nemazee, K. Burki, *Nature* **337**, 562 (1989).
5. M. Okamoto *et al.*, *J. Exp. Med.* **175**, 71 (1992).
6. S. L. Tiegs, D. M. Russell, D. Nemazee, *J. Exp. Med.* **177**, 1009 (1993).
7. C. Chen, E. L. Prak, M. Weigert, *Immunity* **6**, 97 (1997).
8. R. Pelanda *et al.*, *Immunity* **7**, 765 (1997).
9. C. Coleclough, R. P. Perry, K. Karjalainen, M. Weigert, *Nature* **290**, 372 (1981).
10. M. W. Retter, D. Nemazee, *J. Exp. Med.* **188**, 1231 (1998).
11. T. Yamagami, E. ten Boekel, J. Andersson, A. Rolink, F. Melchers, *Immunity* **11**, 317 (1999).
12. Supplemental material is available at *Science* Online (www.sciencemag.org/cgi/content/full/291/5508/1541/DC1).
13. E. Sonoda *et al.*, *Immunity* **6**, 225 (1997).
14. $B220^+mCκ^+$ cells were isolated by cell sorting using a FACSVantage instrument (Beckton Dickinson) to greater than 99% purity. cDNA was synthesized from total RNA using random hexamers and SuperScript II (Gibco BRL). Vκ-Jκs were then amplified in a reverse transcription polymerase chain reaction with the following primers: 3′ primer mCκ: ACGCCATTTTGTCGTTCACTGCCA (for $Igκ^{m/h}$, $IgH^{3H9/+}Igκ^{Vκ4/h}$, $Igκ^{αHEL/h}$, and $Igκ^{Vκ4/h}$ mice) or hCκ: GAGTTACCCGATTGGAGGGCGTTA ($Igκ^{m/h}$) and a 5′ universal primer.
15. D. Allen, T. Simon, F. Sablitzky, K. Rajewsky, A. Cumano, *EMBO J.* **7**, 1995 (1988).
16. M. Hertz, D. Nemazee, *Immunity* **6**, 429 (1997).
17. U. Braun, K. Rajewsky, R. Pelanda, *Proc. Natl. Acad. Sci. U.S.A.* **97**, 7429 (2000).
18. V. Kouskoff, G. Lacaud, K. Pape, M. Retter, D. Nemazee, *Proc. Natl. Acad. Sci. U.S.A.* **97**, 7435 (2000).
19. T. I. Novobrantseva *et al.*, *J. Exp. Med.* **189**, 75 (1999).
20. D. Opstelten, D. G. Osmond, *J. Immunol.* **131**, 2635 (1983).
21. R. R. Hardy, C. E. Carmack, S. A. Shinton, J. D. Kemp, K. Hayakawa, *J. Exp. Med.* **173**, 1213 (1991).
22. D. M. Allman, S. E. Ferguson, V. M. Lentz, M. P. Cancro, *J. Immunol.* **151**, 4431 (1993).
23. B. Rocha *et al.*, *Eur. J. Immunol.* **20**, 1697 (1990).
24. Data from $Igκ^{h/m}$ and $Igκ^{αHEL/h}$ mice were subjected to linear regression analysis, and the entry point for each of the populations was calculated on the basis of the regression formula $y = Bx - A$. The equations obtained were as follows: $Igκ^{h/m}$ hCκ population, $y = 1.44x - 6.33$, entry point [4.4, 0]; mCκ population, $y = 1.40x - 6.35$, entry point [4.5, 0]; $Igκ^{αHEL/h}$ hCκ population, $y = 2.34x - 10.8$, entry point [4.61, 0]; mCκ population, $y = 5.29x - 13.6$, entry point [2.57, 0]. Three mice were killed for each time point.
25. W. Yu *et al.*, *Science* **285**, 1080 (1999).
26. U. Grawunder *et al.*, *Immunity* **3**, 601 (1995).
27. C. Chen *et al.*, *Nature* **373**, 252 (1995).
28. S. B. Harley *et al.*, *Cell* **72**, 325 (1993).
29. D. Melamed, D. Nemazee, *Proc. Natl. Acad. Sci. U.S.A.* **94**, 9267 (1997).
30. R. Pelanda, S. Schaal, R. M. Torres, K. Rajewsky, *Immunity* **5**, 229 (1996).
31. E. L. Prak, M. Weigert, *J. Exp. Med.* **182**, 541 (1995).
32. Lak27 (anti-3-83) was raised in an Igκ-deficient mouse immunized with the 3-83 antibody.
33. The mCκ cell population from $Igκ^{αHEL/h}$ mice consists of unedited VκαHEL expressors, as well as a small number of cells (8.5%, Table 1) that have edited the targeted light chain on the mCκ allele. This population would not be seen in our assay. Although not shown in Fig. 2, $BrdU^+λ^+$ cells appeared in the immature compartment after 24 hours of BrdU injection [H. Arakawa, T. Shimizu, S. Takeda, *Int. Immunol.* **8**, 91 (1996)].

34. We thank M. Weigert for $Igκ^{Vκ4}$ and $Igκ^{Vκ8}$ mice, and members of the Nussenzweig lab for suggestions. Supported by grants from Deutsche Forschungsgemeinschaft through SFB 243 (K.R.), by NIH grant 33890 (M.C.N.), and by an NSF predoctoral fellowship (R.C.). M.C.N. is a Howard Hughes Medical Institute investigator.

16 October 2000; accepted 4 January 2001

Induction of Direct Antimicrobial Activity Through Mammalian Toll-Like Receptors

Sybille Thoma-Uszynski,[1]* Steffen Stenger,[2]* Osamu Takeuchi,[3] Maria Teresa Ochoa,[1] Matthias Engele,[2] Peter A. Sieling,[1] Peter F. Barnes,[4] Martin Röllinghoff,[2] Pal L. Bölcskei,[5] Manfred Wagner,[5] Shizuo Akira,[3] Michael V. Norgard,[6] John T. Belisle,[7] Paul J. Godowski,[8] Barry R. Bloom,[9] Robert L. Modlin[1]†

The mammalian innate immune system retains from *Drosophila* a family of homologous Toll-like receptors (TLRs) that mediate responses to microbial ligands. Here, we show that TLR2 activation leads to killing of intracellular *Mycobacterium tuberculosis* in both mouse and human macrophages, through distinct mechanisms. In mouse macrophages, bacterial lipoprotein activation of TLR2 leads to a nitric oxide–dependent killing of intracellular tubercle bacilli, but in human monocytes and alveolar macrophages, this pathway was nitric oxide–independent. Thus, mammalian TLRs respond (as *Drosophila* Toll receptors do) to microbial ligands and also have the ability to activate antimicrobial effector pathways at the site of infection.

The primitive immune system of *Drosophila* has evolved to be highly efficient at combating microbial pathogens, largely through a family of cell-surface receptors known as Toll. The activation of Toll proteins by microbial ligands triggers an intracellular signaling pathway involving nuclear factor κB (NF-κB) homologs that leads to the transcription of genes encoding antimicrobial proteins (*1–3*). The *Drosophila* Toll system is structurally conserved and homologous to the mammalian TLR family (*4*). Microbial ligands, including lipopolysaccharide (LPS) and bacterial lipoproteins, have been shown to activate mammalian TLRs, facilitating transcription of genes that regulate the adaptive response, including cytokines and costimulatory molecules (*4–10*). It remains unclear, however, whether activation of mammalian TLRs triggers direct antimicrobial effector pathways.

We initially investigated whether activation of mouse macrophages by bacterial lipoproteins reduced the viability of intracellular *Mycobacterium tuberculosis* (*11*). The 19-kD lipoprotein of *M. tuberculosis* (*8*) or the Tp47 lipopeptide of *Treponema pallidum* reduced the viability of intracellular *M. tuberculosis* in a murine macrophage-like cell line, RAW264.7, by up to 70%, as measured by colony-forming units (CFUs) (Web fig. 1) (*11, 12*). The induction of inducible nitric oxide synthase (iNOS) and release of nitric oxide (NO) represent a powerful antimycobacterial defense mechanism in mice (*13–15*). Because bacterial lipoproteins induce iNOS promoter activity (*8*), we hypothesized that the antimicrobial activity observed after cellular activation with lipoproteins could be mediated through TLR-induced NO production. *M. tuberculosis*–infected RAW cells were stimulated with the 19-kD lipoprotein in the presence or absence of pharmacologic inhibitors of iNOS (*11*) and assayed for NO production (*16*) and antimicrobial activity. We found that the production of NO was almost completely suppressed in the presence of L-N^6-(1-iminoethyl)-lysine (L-NIL) or L-N^6-nitroarginine-methyl ester (L-NAME), but not the inactive enantiomer D-NAME (Fig. 1A, left). Concomitantly, inhibition of NO production abrogated the antimicrobial activity induced by the 19-kD lipoprotein (Fig. 1A, right), demonstrating the requirement for NO in TLR-mediated antimicrobial responses.

To establish that the lipoprotein-induced antimicrobial activity is dependent on TLR activation, we tested the ability of the 19-kD protein to activate the antimicrobial pathway of peritoneal macrophages from TLR2-deficient ($TLR2^{-/-}$) or TLR4-deficient ($TLR4^{-/-}$) mice (*17*). Experiments were performed with uninfected [Web fig. 2 (*12*)] and *M. tuberculosis*–infected (Fig. 1B) macrophages. Primary peritoneal macrophages from $TLR2^{-/-}$ mice responded only marginally in production of NO in response to the 19-kD protein and did not appreciably reduce the viability of intracellular *M. tuberculosis* compared with wild-type macrophages (Fig. 1B). This result establishes that activation of TLR2 on murine macrophages leads to NO-dependent growth inhibition of intracellular *M. tuberculosis*.

The question of whether human macro-

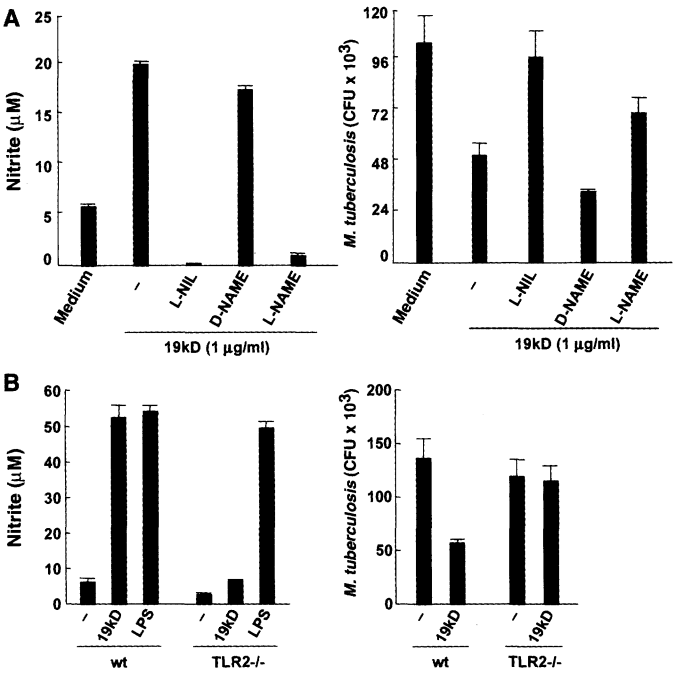

Fig. 1. Microbial lipoproteins trigger growth inhibition of intracellular *M. tuberculosis*. (**A**) The 19-kD lipoprotein of *M. tuberculosis* mediates an NO-independent antimicrobial activity in RAW cells. The CFUs were determined 48 hours after infection of RAW cells with an MOI of 5. The inhibitors (L-NIL, 1 mM; L-NAME, 2 mM) were added to the infected cells immediately after the end of the pulse infection, together with the 19-kD lipoprotein (1 μg/ml). The figures represent the average ± SEM of three or more independent experiments. (**B**) Lipoprotein-induced killing of *M. tuberculosis* is mediated by TLR2. Thioglycollate-elicited macrophages from control (wt) and gene-deleted ($TLR2^{-/-}$) mice were infected with *M. tuberculosis* at an MOI of 5. Production of NO (Griess reaction) and bacterial load (plating of cell lysates) were determined 48 hours after addition of the 19-kD lipoprotein (1 μg/ml) or LPS (0.1 μg/ml). The figure shows the average of one experiment ± SEM performed in triplicate.

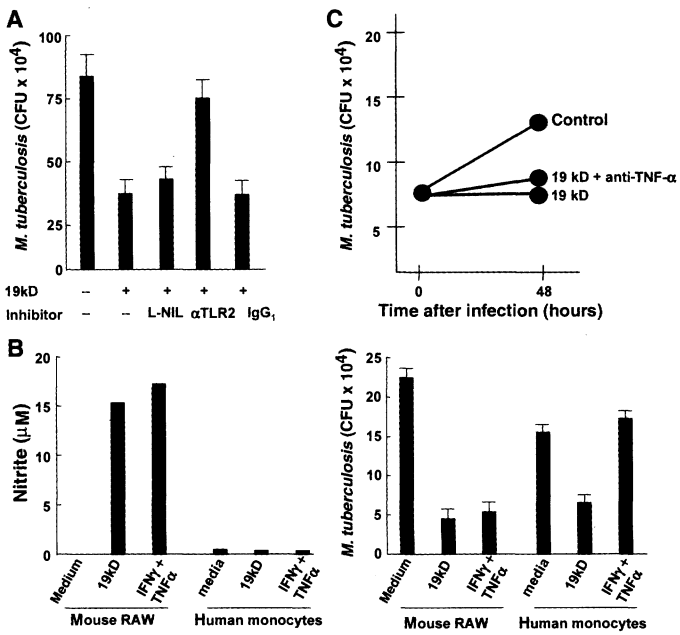

Fig. 2. Primary human cells kill *M. tuberculosis* via a TLR2-dependent, but NO-independent, pathway. (**A**) Inhibition of mycobacterial growth in human monocytes is inhibited in the presence of a blocking antibody to TLR2 (αTLR2), but is independent of NO production. Infected monocytes (MOI 5) were cultured in the presence of an antibody against TLR2 (10 μg/ml) or L-NIL (1 mM) for 48 hours, and intracellular growth was determined by plating serial dilutions of cell lysates in duplicates. (**B**) TNF-α and IFN-γ induce the production of NO and antibacterial activity in mouse macrophages, but not in human monocytes. TNF-α and IFN-γ (both at 10 ng/ml) were added to infected murine macrophages (RAW) or human monocytes. NO release and bacterial viability were determined after 48 hours. The figures show the average of four independent experiments ± SEM using cells from different donors. (**C**) Antimycobacterial activity of the 19-kD lipoprotein is TNF-independent. The 19-kD lipoprotein (2 μg/ml) and antibodies against TNF (anti-TNF-α, 20 μg/ml) were added as indicated. Cells were lysed after 48 hours, and the number of CFUs were determined.

[1]Division of Dermatology, Department of Microbiology and Immunology and Molecular Biology Institute, UCLA School of Medicine, Los Angeles, CA 90095, USA. [2]Institute for Clinical Microbiology, Immunology and Hygiene, Universität Erlangen, 91054 Erlangen, Germany. [3]Department of Host Defense, Osaka University, Osaka, Japan. [4]Center for Pulmonary and Infectious Disease Control, Departments of Medicine, Cell Biology, and Immunology, University of Texas Health Center, Tyler, TX 75708–3154, USA. [5]Klinikum Nürnberg, Medical Clinic 3, 90419 Nürnberg, Germany. [6]University of Texas Southwestern Medical Center, Dallas, TX 75235, USA. [7]Department of Microbiology, Colorado State University, Fort Collins, CO 80523, USA. [8]Department of Molecular Biology, Genentech, South San Francisco, CA 94080, USA. [9]Office of the Dean, Harvard School of Public Health, Boston, MA 02115, USA.

*These authors contributed equally to this work.
†To whom correspondence should be addressed. E-mail: rmodlin@mednet.ucla.edu

phages exert antimicrobial activity through NO remains highly controversial, and we sought to ascertain whether they did so after activation of TLRs. Activation of human monocytes with bacterial lipoproteins reduced the viability of intracellular *M. tuberculosis* to an extent comparable in magnitude to that found in activated mouse macrophages (Web fig. 3) (*12*, *18*). The killing of intracellular *M. tuberculosis* in human monocytes was clearly dependent on lipoprotein activation via TLR2, because a monoclonal antibody against TLR2 (*8*, *9*) blocked the reduction in CFUs by greater than 90% (Fig. 2A). In striking contrast to mouse macrophages, the addition of the iNOS inhibitor, L-NIL, failed to block the 19-kD lipoprotein–induced killing of intracellular *M. tuberculosis*. This correlated with the failure of the 19-kD lipoprotein to induce production of NO in human monocytes (Fig. 2B). This observation was extended by use of another potent stimulus known to induce NO in mouse macrophages, the combination of tumor necrosis factor–α (TNF-α) and interferon-γ (IFN-γ) (*19*) (Fig. 2B). In mouse RAW cells, TNF-α plus IFN-γ induced the production of NO and reduced the viability of intracellular *M. tuberculosis* to an extent equivalent to the effect of the 19-kD lipoprotein. In contrast, in human monocyte-derived macrophages, the combination of TNF-α plus IFN-γ neither induced detectable NO production nor exerted any antimicrobial effect, but did induce cytokine release. TNF-α has been shown to induce growth inhibition of avirulent *M. tuberculosis* in human macrophages (*20*), but we found it to support the growth of virulent *M. tuberculosis* in these cells (*21*). Furthermore, the addition of antibodies against TNF-α did not abrogate the antimicrobial activity of the 19-kD lipoprotein against the virulent form used in this study (Fig. 2C). Taken together, these data indicate that TLR2 activation in human monocytes induces a powerful antimicrobial activity that is independent of NO and TNF-α.

The ability of alveolar macrophages (AMs) to kill *M. tuberculosis* represents a critical local defense mechanism in determining the outcome of tuberculosis infection in the lung. Alveolar macrophages were isolated from bronchoalveolar lavage, infected with *M. tuberculosis* (*22*), and stimulated with the *M. tuberculosis* 19-kD lipoprotein, then survival of the bacteria was determined. Stimulation of infected AMs with lipoprotein induced an antimicrobial response that was independent of NO release, but dependent on TLR2 signaling (Fig. 3A). Consistent with the failure of the specific iNOS inhibitor L-NIL to inhibit antibacterial activity, AMs infected with mycobacteria failed to secrete detectable amounts of NO in vitro. Although it has been reported that AMs can express iNOS (*23*), these results further indicate that a mechanism independent of NO contributes to their microbicidal activity. The presence of TLR2 on cells of the monocyte/macrophage lineage in lesions of tuberculosis infection indicates that activation of TLR2 could contribute to host defense at the site of disease activity (Fig. 3B and Web figs. 4 and 5) (*24*).

Throughout millions of years of evolution, the immune system, from insects to mammals, has retained the structure of Toll receptors, as well as an NF-κB signaling pathway, as an innate mechanism to respond to threats from microbial pathogens. The present results indicate that the mouse and human TLR pathway has similarly retained the ability to activate direct antimicrobial effector mechanisms, although the pathways are distinct. Whereas, in mice, TLR activation leads to an NO-dependent antimicrobial pathway, in humans the TLR-activated antimicrobial pathway is NO-independent. In *Drosophila*, activation of Toll leads to the induction of a variety of antimicrobial peptides, including metchnikowan, defensins, cecropins, and drosomycin (*1*–*3*). The present study suggests that a detailed investigation of the TLR2-dependent antimicrobial effector mechanisms in human cells of the monocyte/macrophage lineage is warranted. The clues from *Drosophila* suggest that exploring induction of antimicrobial peptides in these cells could be fruitful (*25*). Knowledge arising from such investigation should provide new insights into mechanisms of innate immunity in humans.

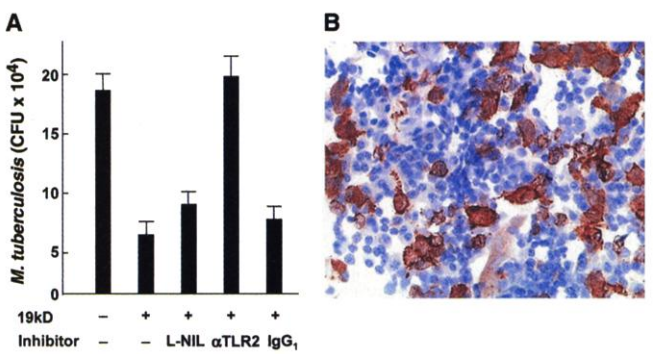

Fig. 3. TLR2 is expressed at the site of infection in human tuberculosis. **(A)** Activation of AMs by the 19-kD lipoprotein reduces the viability of intracellular *M. tuberculosis* by a TLR2-dependent, NO-independent mechanism. AMs were infected with *M. tuberculosis* (MOI 2) for 4 hours, and the 19-kD lipoprotein (1 μg/ml) or the inhibitors were added. Bacterial growth was determined after 48 hours. The graph shows one representative experiment of four using cells from different donors and are expressed as CFUs ± SEM. **(B)** TLR2 expression in tuberculous lymphadenitis by immunoperoxidase. Photomicrograph (40× objective) demonstrates the presence of TLR2 (red label) on large ovoid cells within granulomas, typical of cells of the monocyte/macrophage lineage.

References and Notes

1. B. Lemaitre, E. Nicolas, L. Michaut, J. M. Reichhart, J. A. Hoffmann, *Cell* **86**, 973 (1996).
2. B. Lemaitre, J. M. Reichhart, J. A. Hoffmann, *Proc. Natl. Acad. Sci. U.S.A.* **94**, 14614 (1997).
3. J. A. Hoffmann, F. C. Kafatos, C. A. Janeway, R. A. B. Ezekowitz, *Science* **284**, 1313 (1999).
4. R. Medzhitov, P. Preston-Hurlburt, C. A. Janeway, *Nature* **388**, 394 (1997).
5. R. B. Yang *et al.*, *Nature* **395**, 284 (1998).
6. C. J. Kirschning, H. Wesche, T. M. Ayres, M. Rothe, *J. Exp. Med.* **188**, 2091 (1998).
7. A. Poltorak *et al.*, *Science* **282**, 2085 (1998).
8. H. D. Brightbill *et al.*, *Science* **285**, 732 (1999).
9. A. O. Aliprantis *et al.*, *Science* **285**, 736 (1999).
10. D. M. Underhill *et al.*, *Nature* **401**, 811 (1999).
11. RAW264.7 cells (ATCC, Manassas, VA) or human adherent cells were infected with *M. tuberculosis* [multiplicity of infection (MOI) 5 for 4 hours], as described (*26*, *27*) and coincubated with the microbial ligand 19-kD *M. tuberculosis* lipoprotein (*8*) or the Tp47 lipopeptide for 48 hours. Subsequently, cells were lysed, and the CFUs were assessed. In addition, experiments were performed in the presence of inhibitors of iNOS, L-NIL, L-NAME or D-NAME (Sigma).
12. Supplementary material is available on *Science* Online at www.sciencemag.org/cgi/content/full/291/5508/1544/DC1
13. J. Chan, Y. Xing, R. S. Magliozzo, B. R. Bloom, *J. Exp. Med.* **175**, 1111 (1992).
14. J. D. MacMicking *et al.*, *Proc. Natl. Acad. Sci. U.S.A.* **94**, 5243 (1997).
15. J. Chan, K. Tanaka, D. Carroll, J. Flynn, B. R. Bloom, *Infect. Immun.* **63**, 736 (1995).
16. Y. Vodovotz, C. Bogdan, J. Paik, Q. W. Xie, C. Nathan, *J. Exp. Med.* **178**, 605 (1993).
17. O. Takeuchi *et al.*, *Immunity* **11**, 443 (1999).
18. Adherent cells were prepared from normal donors and contained >95% monocytes, as confirmed by fluorescence-activated cell sorting (FACS) staining. For blocking experiments, *M. tuberculosis*–infected cells were stimulated with ligand in the presence of a monoclonal antibody directed against TLR2 (*8*, *9*) (10 μg/ml), a neutralizing antibody against TNF-α (20 μg/ml, R&D Systems) or an isotype control.
19. S. Stenger, W. Solbach, M. Röllinghoff, C. Bogdan, *Eur. J. Immunol.* **21**, 1669 (1991).
20. C. S. Hirsch, J. J. Ellner, D. G. Russell, E. A. Rich, *J. Immunol.* **152**, 743 (1994).
21. M. Engele, E. Stössel, M. Wagner, P. Bölcskei, M. Röllinghoff, S. Stenger, manuscript in preparation.
22. Alveolar macrophages were isolated from bronchoalveolar lavage samples from patients with conditions other than tuberculosis. Lavage fluid was filtered through a cell strainer (Becton Dickinson). Adherent cells were depleted of remaining lymphocytes by immunomagnetic depletion (CD3, CD19, CD56), and the resulting population contained >98% AMs as determined by α-naphthyl acetate esterase staining (Sigma).
23. S. Nicholson *et al.*, *J. Exp. Med.* **183**, 2293 (1996).
24. Lymph node specimens were obtained from five tuberculosis patients after informed consent. Single immunoperoxidase labeling using a monoclonal antibody against TLR2 was performed as described (*28*).

25. Although the kinetic analysis of the effect of lipoproteins on the number of CFUs of *M. tuberculosis* does not differentiate between microbicidal and microbiostatic mechanisms [Web fig. 6 (*12*)], antimicrobial proteins can mediate activity by either mechanism. Although it is well known that defensins clearly lyse microbial pathogens in vitro, in vivo, inside a cell, it appears that the principal action is growth inhibition (*29*). Over time, the cumulative effect would be to cause death and elimination of the organism. As the infection is contained, T cell responses, including the release of granulysin (*27*), could contribute to killing of the organism.
26. S. Stenger *et al.*, *Science* **276**, 1684 (1997).
27. S. Stenger *et al.*, *Science* **282**, 121 (1998).
28. D. Jullien *et al.*, *J. Immunol.* **158**, 800 (1997).
29. M. A. Couto, L. Liu, R. I. Lehrer, T. Ganz, *Infect. Immun.* **62**, 2375 (1994).

30. This work was supported in part by grants from the National Institutes of Health (AI 22553, AR 40312, AI 47868, AI 07118), the Deutsche Forschungsgemeinschaft (SFB263), and the AIDS Stipendienprogramm of the Ministry of Science and Technology (BMFT), Germany.

8 December 2000; accepted 16 January 2001

Requirement of a Centrosomal Activity for Cell Cycle Progression Through G_1 into S Phase

Edward H. Hinchcliffe,[1] Frederick J. Miller,[1] Matthew Cham,[1] Alexey Khodjakov,[2] Greenfield Sluder[1]*

Centrosomes were microsurgically removed from BSC-1 African green monkey kidney cells before the completion of S phase. Karyoplasts (acentrosomal cells) entered and completed mitosis. However, postmitotic karyoplasts arrested before S phase, whereas adjacent control cells divided repeatedly. Postmitotic karyoplasts assembled a microtubule-organizing center containing γ-tubulin and pericentrin, but did not regenerate centrioles. These observations reveal the existence of an activity associated with core centrosomal structures—distinct from elements of the microtubule-organizing center—that is required for the somatic cell cycle to progress through G_1 into S phase. Once the cell is in S phase, these core structures are not needed for the G_2-M phase transition.

The centrosome in mammalian cells consists of a pair of centrioles associated with a cloud of pericentriolar material containing the γ-tubulin ring complexes that nucleate microtubules during interphase and mitosis (*1*). The centrioles, along with their associated structures, represent "core centrosomal structures" that determine the precise one-to-two duplication of the centrosome in preparation for mitosis (*2*). After removal of the centrosome, both somatic and embryonic cells can regenerate a microtubule-organizing center (MTOC) (*3–5*) but do not regenerate centrioles (*2, 4*), even though the cytoplasm (in the case of zygotes) contains enough subunits to assemble many complete centrosomes (*6*).

It has been generally understood that both the duplication of the centrosome and variations in its microtubule-nucleating capacity are driven by cell cycle–dependent changes in the cytoplasmic environment (*7*). The notion that the centrosome is a necessary participant in cell cycle progression through interphase was raised by a report that BSC-1 African green monkey karyoplasts (acentrosomal cells) do not enter mitosis even though they grow to larger than normal size (*4*). This finding, coupled with the observation that cyclin-dependent kinase 1–cyclin B (Cdk1-B) is concentrated at the centrosome (*8*), led to the proposals that the presence or duplication (or both) of an intact centrosome is required for the activation of Cdk1-B and entry into mitosis (*4, 9*). However, these proposals lacked direct experimental support because the karyoplasts were not continuously followed in vivo.

To investigate the role of the centrosome in cell cycle progression, we physically cut BSC-1 cells during interphase between the nucleus and the centrosome to form karyoplasts (*4, 10*) and continuously followed the karyoplasts for several days by time-lapse videomicroscopy (*11*). The fact that the centrosome is slightly separated from the nucleus and lies at the center of a mass of granules makes this cell type favorable for this microsurgery (*12*). We brought the microneedle down at the edge of the nucleus, which displaced the centrosome from the nucleus and segregated it into the anucleate cytoplast as the needle approached the cover slip (Fig. 1A). In no case did we cut or fragment the nucleus. Although we cannot know at what point in the cell cycle the cells were cut, 5-bromo-2′-deoxyuridine (BrdU) incorporation experiments (*13*) revealed that they were cut before the completion of S phase (*14*), consistent with previous findings (*4*). None were cut in early G_1 or in prophase.

During the first 1 to 3 hours after the operation, the cytoplasmic granules became organized into a spherical mass at the center of the cytoplast, indicative of the presence of the centrosome, while the granules in the karyoplast remained randomly distributed in the vicinity of the nucleus (Fig. 1B). Normally we removed the cytoplast with the microneedle so that it would not interfere with observations of karyoplast behavior. Within an hour of the microsurgery, karyoplasts extended lamellipodia and resumed movement across the cover slip (Fig. 2A). Later, they grew in area and regenerated their Golgi apparatus to control levels, as judged by in vivo labeling with Bodipy FL C_5-ceramide (*4, 12, 15*).

In 37 experiments, 32 karyoplasts entered mitosis (Fig. 2A), four remained in interphase until the recordings were terminated 24 hours after the microsurgery, and one died within 12 hours. The interval from the microsurgical operation to the onset of mitosis was on average 12.5 hours (range 4 to 24 hours), which is within the normal interphase duration for control cells in our preparations (average 15.5 hours, range 11 to 26 hours, N = 25). In mitosis, karyoplasts aligned chromosomes into a metaphase plate, separated two groups of chromosomes in anaphase, and formed a cleavage furrow (*14*). This indicates that karyoplasts organized a functional, albeit acentrosomal, bipolar spindle [see also (*5, 16*)]. Karyoplasts spent a longer and a more variable amount of time in mitosis (average 197 min, range 68 to 557 min) than did control cells (average 56 min, range 24 to 99 min; N = 40), presumably because of the need for extra time to organize an acentrosomal spindle. In telophase all karyoplasts initiated bipolar cleavage. However, in 13 of 32 cases (41%), the cleavage furrow regressed and the karyoplasts exited mitosis as a single cell with one or more nuclei (*12, 17*).

We unexpectedly found that in 28 of 32 experiments, the postmitotic karyoplasts—whether they divided or not—arrested in interphase for the duration of the observations, up to 60 hours after mitosis (Fig. 2A) (*12*). This was not attributable to loss of cell viability in our preparations, because the karyoplasts showed continuous lamellipod extension, cell motility, and movement of phase-dense granules toward

[1]Department of Cell Biology, University of Massachusetts Medical School, Worcester, MA 01605, USA. [2]Laboratory of Cell Regulation, Wadsworth Center, Albany, NY 12201, USA.

*To whom correspondence should be addressed. E-mail: greenfield.sluder@umassmed.edu